

Ab initio Derivation of Low-Energy Model for Iron-Based Superconductors LaFeAsO and LaFePO

Kazuma NAKAMURA^{1*}, Ryotaro ARITA^{1,2}, and Masatoshi IMADA^{1,2}

¹ Department of Applied Physics, University of Tokyo, 7-3-1 Hongo, Bunkyo-ku, Tokyo 113-8656, Japan

² CREST, JST, 7-3-1 Hongo, Bunkyo-ku, Tokyo 113-8656, Japan

(Received November 8, 2021)

Effective Hamiltonians for LaFeAsO and LaFePO are derived from the downfolding scheme based on first-principles calculations and provide insights for newly discovered superconductors in the family of $\text{LnFeAsO}_{1-x}\text{F}_x$, $\text{Ln} = \text{La, Ce, Pr, Nd, Sm, and Gd}$. Extended Hubbard Hamiltonians for five maximally localized Wannier orbitals per Fe are constructed dominantly from five-fold degenerate iron-3d bands. They contain parameters for effective Coulomb and exchange interactions screened by the polarization of other electrons away from the Fermi level. The onsite Coulomb interaction estimated as 2.2-3.3 eV is compared with the transfer integrals between the nearest-neighbor Fe-3d Wannier orbitals, 0.2-0.3 eV, indicating moderately strong electron correlation. The Hund's rule coupling is found to be 0.3-0.6 eV. The derived model offers a firm basis for further studies on physics of this family of materials. The effective models for As and P compounds turn out to have very similar screened interactions with slightly narrower bandwidth for the As compound.

KEYWORDS: first-principles calculation, effective Hamiltonian, downfolding, constrained RPA method, LaFeAsO, LaFePO, Oxypnictide, high-temperature superconductivity

Recent discovery of a new superconductor, LaFeAs(O,F),¹⁾ has triggered extensive studies on the family of layered iron arsenide compounds with ZrCuSiAs-type or ThCr₂Si₂-type structure, whose superconducting critical temperature T_c is now raising up to ~ 55 K.²⁾ A mother compound LaFeAsO shows antiferromagnetic order³⁾ with bad metallic transport properties¹⁾ supporting a significant role of electron correlations. The antiferromagnetic ordered moment $\sim 0.36 \mu_B$ is unexpectedly small, implying large quantum fluctuations arising from electron correlations with competing ground states. Superconductivity appears when carriers are doped by the substitution of F for O,¹⁾ or the introduction of O vacancies.⁴⁾ Many of experimental data support a significant role of electron correlation in realizing the superconductivity.⁵⁻⁸⁾ Although the As compounds have the maximum $T_c \sim 56$ K, the P compounds show one order of magnitude lower T_c .⁹⁾

Conventional density-functional calculations with the local density approximation (LDA) or the generalized gradient approximation (GGA) have clarified entangled ten-band structure near the Fermi level mainly originating from five-fold degenerate iron-3d orbitals contained in each of two iron atoms in the unit cell.¹⁰⁻¹⁴⁾ For the mother material, the initial LDA calculation¹⁰⁾ predicted the nonmagnetic ground state in close proximity to a ferromagnetic metal while the recent results show antiferromagnetic order.¹¹⁻¹³⁾ In particular, the stripe-type antiferromagnetic order is correctly reproduced.^{12,13)} The calculated ordered moment obtained so far ranges between 1.2 and 2.6 μ_B ,^{11-13,15)} in contrast to the tiny ordered moment discussed above. Broad peak structures of magnetic Lindhard function calculated by using the LDA/GGA Fermi surface suggest competitions of sev-

eral different ordering tendencies.^{14,16-18)}

Although overall experimental results suggest noticeable correlation effects, realistic roles of electron correlations on theoretical grounds are not clear. The relevance of the correlation effect is under active debates.¹⁹⁻²¹⁾ It is imperative to estimate at least the effective Coulomb interaction from first principles. Furthermore, since all the 3d bands of Fe are as a first look wholly involved near the Fermi level, it is important to elucidate interplay of orbital degeneracy and electron correlation, which can be studied only by a model for degenerate bands. A reliable theoretical model derived for this family of compounds thus provides us with a firm basis for understanding the superconductivity and also a starting point for exploring further possibility of higher T_c compounds.

In this letter, we present *ab initio* low-energy effective Hamiltonians of LaFeAsO and LaFePO. Implications for the superconductivity in F-doped materials are also discussed. A reliable downfolding scheme has recently been established which has enabled derivation of low-energy effective Hamiltonians from *ab initio* density-functional calculation of real materials.²²⁻²⁴⁾ The low-energy Hamiltonian is derived after eliminating higher-energy degrees of freedom and estimating the renormalization effect from the high-energy part onto the bands near the Fermi level. The accuracy of the downfolding procedure has been established in various cases.²⁴⁻²⁶⁾ Here, we employ this downfolding scheme in deriving the extended Hubbard models of LaFeAsO and LaFePO, consisting of band dispersion (kinetic energy) of electrons at maximally localized Wannier orbitals (MLWOs),²⁷⁾ as well as screened Coulomb and exchange interactions. Since the ten-fold Fe-3d bands are basically isolated from other bands, we derive effective models for these ten bands.

*Electronic mail: kazuma@solis.t.u-tokyo.ac.jp

The extended ten-band Hubbard model reads

$$\begin{aligned} \mathcal{H} = & \sum_{\sigma} \sum_{\mathbf{R}\mathbf{R}'} \sum_{nm} t_{m\mathbf{R}n\mathbf{R}'} a_{n\mathbf{R}}^{\sigma\dagger} a_{m\mathbf{R}'}^{\sigma} \\ & + \frac{1}{2} \sum_{\sigma\rho} \sum_{\mathbf{R}\mathbf{R}'} \sum_{nm} \left\{ U_{m\mathbf{R}n\mathbf{R}'} a_{n\mathbf{R}}^{\sigma\dagger} a_{m\mathbf{R}'}^{\rho\dagger} a_{m\mathbf{R}'}^{\rho} a_{n\mathbf{R}}^{\sigma} \right. \\ & \left. + J_{m\mathbf{R}n\mathbf{R}'} (a_{n\mathbf{R}}^{\sigma\dagger} a_{m\mathbf{R}'}^{\rho\dagger} a_{n\mathbf{R}}^{\rho} a_{m\mathbf{R}'}^{\sigma} + a_{n\mathbf{R}}^{\sigma\dagger} a_{m\mathbf{R}'}^{\rho\dagger} a_{m\mathbf{R}'}^{\rho} a_{n\mathbf{R}}^{\sigma}) \right\}, \end{aligned} \quad (1)$$

where $a_{n\mathbf{R}}^{\sigma\dagger}$ ($a_{n\mathbf{R}}^{\sigma}$) is a creation (annihilation) operator of an electron with spin σ in the n th MLWO centered on Fe atoms in the unitcell at \mathbf{R} . $t_{m\mathbf{R}n\mathbf{R}'}$ contains single-particle levels and transfer integrals, given by $t_{m\mathbf{R}n\mathbf{R}'} = \langle \phi_{m\mathbf{R}} | \mathcal{H}_0 | \phi_{n\mathbf{R}'} \rangle$ with $|\phi_{n\mathbf{R}}\rangle = a_{n\mathbf{R}}^{\dagger} |0\rangle$ and \mathcal{H}_0 being the one-body part of \mathcal{H} . $U_{m\mathbf{R}n\mathbf{R}'}$ and $J_{m\mathbf{R}n\mathbf{R}'}$ are screened Coulomb and exchange interactions, respectively, expressed as

$$U_{m\mathbf{R}n\mathbf{R}'} = \langle \phi_{m\mathbf{R}} \phi_{m\mathbf{R}} | W | \phi_{n\mathbf{R}'} \phi_{n\mathbf{R}'} \rangle \quad (2)$$

and

$$J_{m\mathbf{R}n\mathbf{R}'} = \langle \phi_{m\mathbf{R}} \phi_{n\mathbf{R}'} | W | \phi_{n\mathbf{R}'} \phi_{m\mathbf{R}} \rangle \quad (3)$$

with W being a screened Coulomb interaction. There are already attempts to estimate $t_{m\mathbf{R}n\mathbf{R}'}$ using MLWO.^{11,14} We here focus on an *ab initio* derivation of the many-body part of \mathcal{H} ; we estimate the interaction parameters in eqs. (2) and (3), based on a constrained random-phase approximation (cRPA).^{22,23} The cRPA has several advantages over other methods such as constrained LDA.²⁸ We can precisely exclude screening processes among the Fe-3d MLWOs being the bases of the effective model. (This screening should be considered when we solve the effective model.) In addition, we can calculate matrix elements of W as a function of \mathbf{R} and \mathbf{R}' ;²⁹ i.e., we can obtain onsite and offsite interactions at one time. The cRPA becomes a good approximation, when the high-energy eliminated bands are well separated from the Fermi level and the screened Coulomb interactions between the high-energy electrons and the low-energy electrons are weak. As is noted above, quantitative accuracies of our downfolding including cRPA has already been confirmed in a number of examples.^{22-25,29} In the present case of the iron compounds, the condition above is equally satisfied.

$U_{m\mathbf{R}n\mathbf{R}'}$ of eq. (2) is practically calculated in the reciprocal space by using a Fourier transform of W ,

$$W(\mathbf{r}, \mathbf{r}') = \sum_{\mathbf{q}\mathbf{G}\mathbf{G}'} e^{i(\mathbf{q}+\mathbf{G})\mathbf{r}} W_{\mathbf{G}\mathbf{G}'}(\mathbf{q}) e^{-i(\mathbf{q}+\mathbf{G}')\mathbf{r}'}. \quad (4)$$

Here, \mathbf{G} is a reciprocal lattice vector and \mathbf{q} is a wave vector in the first Brillouin zone. We define $W_{\mathbf{G}\mathbf{G}'}(\mathbf{q})$ as

$$W_{\mathbf{G}\mathbf{G}'}(\mathbf{q}) = \frac{4\pi}{\Omega} \frac{1}{|\mathbf{q} + \mathbf{G}|} \epsilon_{\mathbf{G}\mathbf{G}'}^{-1}(\mathbf{q}) \frac{1}{|\mathbf{q} + \mathbf{G}'|},$$

where Ω is the crystal volume and $\epsilon_{\mathbf{G}\mathbf{G}'}^{-1}(\mathbf{q})$ is the inverse dielectric matrix which is related to the irreducible polarizability χ by $\epsilon_{\mathbf{G}\mathbf{G}'}(\mathbf{q}) = \delta_{\mathbf{G}\mathbf{G}'} - v(\mathbf{q} + \mathbf{G})\chi_{\mathbf{G}\mathbf{G}'}(\mathbf{q})$, where $v(\mathbf{q}) = 4\pi/\Omega|\mathbf{q}|^2$ is the bare Coulomb interaction.

The polarization matrix $\chi_{\mathbf{G}\mathbf{G}'}(\mathbf{q})$ is calculated as

$$\begin{aligned} \chi_{\mathbf{G}\mathbf{G}'}(\mathbf{q}) = & \sum_{\mathbf{k}} \sum'_{\alpha\beta} \langle \psi_{\alpha\mathbf{k}+\mathbf{q}} | e^{i(\mathbf{q}+\mathbf{G})\mathbf{r}} | \psi_{\beta\mathbf{k}} \rangle \\ & \times \langle \psi_{\beta\mathbf{k}} | e^{-i(\mathbf{q}+\mathbf{G})\mathbf{r}} | \psi_{\alpha\mathbf{k}+\mathbf{q}} \rangle \frac{f_{\alpha\mathbf{k}+\mathbf{q}} - f_{\beta\mathbf{k}}}{E_{\alpha\mathbf{k}+\mathbf{q}} - E_{\beta\mathbf{k}}}, \end{aligned}$$

where $\{\psi_{\alpha\mathbf{k}}\}$ are the Bloch states and the prime attached to the band sum indicates that we exclude the 3d-3d band transitions in the calculation of χ . By inserting eq. (4) into eq. (2), we obtain the form of

$$U_{m\mathbf{0}n\mathbf{R}} = \frac{4\pi}{\Omega} \sum_{\mathbf{q}\mathbf{G}\mathbf{G}'} e^{-i\mathbf{q}\mathbf{R}} \rho_{m\mathbf{q}}(\mathbf{G}) \epsilon_{\mathbf{G}\mathbf{G}'}^{-1}(\mathbf{q}) \rho_{n\mathbf{q}}^*(\mathbf{G}'), \quad (5)$$

where

$$\rho_{n\mathbf{q}}(\mathbf{G}) = \frac{1}{N|\mathbf{q} + \mathbf{G}|} \sum_{\mathbf{k}}^N \langle \tilde{\psi}_{n\mathbf{k}+\mathbf{q}} | e^{i(\mathbf{q}+\mathbf{G})\mathbf{r}} | \tilde{\psi}_{n\mathbf{k}} \rangle$$

with $|\tilde{\psi}_{n\mathbf{k}}\rangle = \sum_{\mathbf{R}}^N |\phi_{n\mathbf{R}}\rangle e^{-i\mathbf{k}\mathbf{R}}$. It should be noted here that the quantities $\langle \tilde{\psi}_{m\mathbf{k}+\mathbf{q}} | e^{i(\mathbf{q}+\mathbf{G})\mathbf{r}} | \tilde{\psi}_{n\mathbf{k}} \rangle$ can be easily evaluated with the fast Fourier transformation technique. Matrix elements of the bare (or unscreened) Coulomb interaction as $U_{m\mathbf{0}n\mathbf{R}}^{\text{bare}} = \langle \phi_{m\mathbf{0}} \phi_{m\mathbf{0}} | v | \phi_{n\mathbf{R}} \phi_{n\mathbf{R}} \rangle$ are calculated with replacing $\epsilon_{\mathbf{G}\mathbf{G}'}^{-1}(\mathbf{q})$ of eq. (5) by $\delta_{\mathbf{G}\mathbf{G}'}$. The parallel treatment is applied to the derivation of screened exchange interactions in eq. (3). The result is

$$J_{m\mathbf{0}n\mathbf{R}} = \frac{4\pi}{\Omega} \sum_{\mathbf{q}\mathbf{G}\mathbf{G}'} \rho_{mn\mathbf{R}\mathbf{q}}(\mathbf{G}) \epsilon_{\mathbf{G}\mathbf{G}'}^{-1}(\mathbf{q}) \rho_{mn\mathbf{R}\mathbf{q}}^*(\mathbf{G}') \quad (6)$$

with

$$\rho_{mn\mathbf{R}\mathbf{q}}(\mathbf{G}) = \frac{1}{N|\mathbf{q} + \mathbf{G}|} \sum_{\mathbf{k}}^N e^{-i\mathbf{k}\mathbf{R}} \langle \tilde{\psi}_{m\mathbf{k}+\mathbf{q}} | e^{i(\mathbf{q}+\mathbf{G})\mathbf{r}} | \tilde{\psi}_{n\mathbf{k}} \rangle.$$

We implemented this scheme in *Tokyo Ab initio Program Package*.³⁰ With this program, electronic-structure calculations with the GGA exchange-correlation functional³¹ were performed using a plane-wave basis set and the Troullier-Martins norm-conserving pseudopotentials³² in the Kleinman-Bylander representation.³³ Our iron pseudopotential was constructed under the reference configuration $(3d)^{6.0}(4s)^{1.8}(4p)^{0.0}$ by employing the cutoff radii for the 3d, 4s, and 4p states at 2.1 Bohr. The energy cutoff was set to 64 Ry and a $9 \times 9 \times 5$ k -point sampling was employed. The experimental crystal-structure data were taken from ref. 3 for LaFeAsO and ref. 9 for LaFePO. The dielectric matrices were expanded in plane waves with an energy cutoff of 64 Ry and the total number of bands included in the sum in eq. (5) was set to 70. The sum of \mathbf{k} in eq. (5) was evaluated by the tetrahedron method. The additional terms in the long-wavelength dielectric matrix due to nonlocal terms in the pseudopotentials was explicitly considered following ref. 34. The point $\mathbf{q} = \mathbf{G} = \mathbf{0}$ in eqs. (5) and (6) requires special handling because of the singularity in the Coulomb interaction, which was treated in the manner described in ref. 34.

The upper two panels of Fig. 1 shows *ab initio* band structures of LaFeAsO (left) and LaFePO (right). We see a good agreement between the original GGA band (red

line) and the Wannier-interpolated band (blue dots). The lower panels visualize our calculated MLWOs with the yz (left) and z^2 (right) symmetry. In principle, the band dispersion thus obtained should be renormalized by the interaction between electrons in the Fe-3d and eliminated bands in the downfolding procedure.²²⁾ In this letter, we assume that this self-energy effect is small and thus we employ the same dispersion for the downfolded Hamiltonian. The overall band structure of LaFeAsO shows a feature similar to that of LaFePO with slightly ($\sim 20\%$) narrower bandwidth for the As compound. Around the Γ point, in addition to two hole cylinders with the d_{yz} and d_{zx} characters, a 2D-like $d_{x^2-y^2}$ band crosses near the Fermi level for the As compound, in contrast to a 3D-like d_{z^2} band of the P compound.

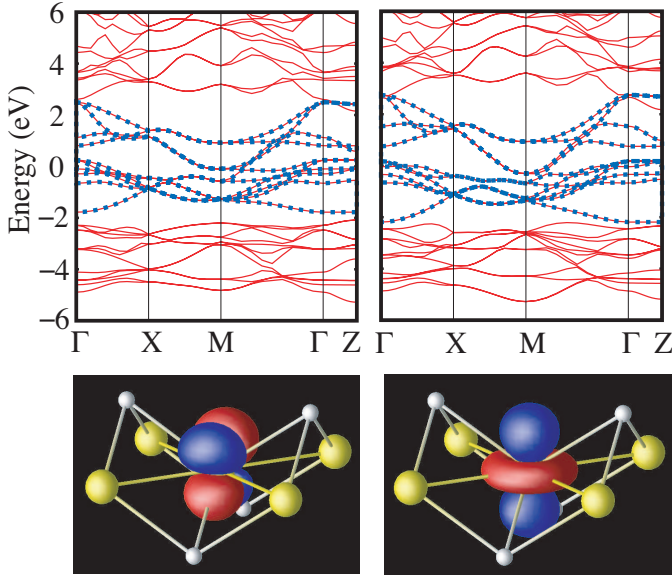


Fig. 1. Upper panels: *Ab initio* band structures of LaFeAsO (left) and LaFePO (right). Red line and Blue dots are original-GGA and Wannier-interpolated bands, respectively. The zero of energy is the Fermi level. Lower panels: Isosurface contours of yz - (left) and z^2 - (right) MLWOs in LaFeAsO. The amplitudes of the contour surface are $+1.5/\sqrt{v}$ (blue) and $-1.5/\sqrt{v}$ (red), where v is the volume of the primitive cell. Fe and As nuclei are illustrated by yellow and silver spheres, respectively.

In Fig. 2, we plot diagonal elements of the macroscopic cRPA dielectric matrix, $\epsilon_M(\mathbf{q} + \mathbf{G}) = 1/\epsilon_{\mathbf{G}\mathbf{G}}^{-1}(\mathbf{q})$, calculated for LaFeAsO, as a function of $|\mathbf{q} + \mathbf{G}|$. We note that the resulting dielectric constant ϵ_M^0 at $\mathbf{q} + \mathbf{G} \rightarrow 0$ exhibits a rather high value of 6.3, which is compared to that of transition metal oxides such as SrVO₃ (6.5). It is also interesting to note that $\epsilon_M(\mathbf{q} + \mathbf{G})$ does not severely depend on the direction of $\mathbf{q} + \mathbf{G}$, which means that the screening response is quite isotropic.

Fig. 3 plots matrix elements of the screened Coulomb interaction, $U_{m0n\mathbf{R}}$ in eq. (5), denoted by green dots, for LaFeAsO as a function of the distance between the centers of the MLWOs; $r = |\langle \phi_{n\mathbf{R}} | \mathbf{r} | \phi_{n\mathbf{R}} \rangle - \langle \phi_{m\mathbf{0}} | \mathbf{r} | \phi_{m\mathbf{0}} \rangle|$. In this plot, we set m to a d_{xy} MLWO and display only the interactions between it and other MLWOs. For comparison, we also plot bare Coulomb interactions

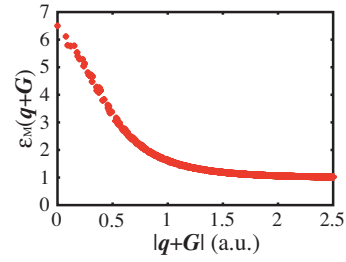


Fig. 2. Macroscopic dielectric function of LaFeAsO as a function of $|\mathbf{q} + \mathbf{G}|$ obtained by the constrained RPA method.

$U_{m0n\mathbf{R}}^{\text{bare}}$ as red dots, which decay as $1/r$ (solid line) beyond the nearest-neighbor Fe-Fe distance ($\geq 2.65 \text{ \AA}$). It is clear that the bare Coulomb interaction is significantly screened. In addition, as expected from Fig. 2, $U_{m0n\mathbf{R}}$ decays as an isotropic function of $1/(\epsilon_M^0 r)$ (dotted line). Since the offsite interactions ($U_{m0n\mathbf{R} \neq 0}$) are more than five times smaller than the onsite U values, we may neglect them in the first step and just start with the onsite Hubbard model. The screened exchange interactions of $J_{m0n\mathbf{R}}$ in eq. (6) are found to decay very quickly; the magnitude is nearly zero, except for the onsite values.

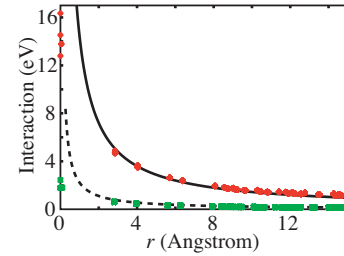


Fig. 3. Calculated screened Coulomb interactions of LaFeAsO as a function of the distance between the centers of MLWOs. Only the interactions between a d_{xy} MLWO at the homecell and other MLWOs are plotted. The red and green dots represent the bare and screened interactions, respectively. The solid and dotted curves denotes $1/r$ and $1/(\epsilon_M^0 r)$, respectively.

We summarize in Table I the list of the important parameters in the low-energy effective Hamiltonian of eq. (1). The transfer integral between nearest-neighbor iron Wannier orbitals, t , is typically 0.2-0.3 eV, whereas the onsite screened Coulomb interaction, U , exhibits 2.2-3.3 eV. The strong orbital dependence comes from the fact that each orbital has different amount of leakage on the neighboring As atoms. The onsite exchange interaction (Hund's rule coupling) is 0.3-0.6 eV. We note that the resulting U and J values are smaller than the bare values by the factors of about 1/5 and 4/5, respectively. We note in passing that, for the two-degenerate d_{yz} and d_{zx} orbitals, our computed $J_{yz,zx}$ ($= 0.45 \text{ eV}$) is close to the value estimated from $(U_{yz,yz} - U_{yz,zx})/2$ (0.50 eV). The interaction parameters for the P compound are found to be very similar; for example, the onsite U values range from 1.9 eV for $d_{x^2-y^2}$ to 3.3 eV for d_{z^2} and d_{xy} as in the case of the As compounds.

The present value of U is substantially smaller than the

Table I. List of important parameters (in eV) in the present extended Hubbard Hamiltonian in eq. (1). From the top, the three 5×5 matrices represent transfer integrals between nearest-neighbor sites, onsite screened Coulomb interactions, and onsite exchange interactions of LaFeAsO. The bottom 5×5 matrix is transfer integrals of LaFePO. The onsite energies for the five orbitals of LaFeAsO are $(\epsilon_{xy}, \epsilon_{yz}, \epsilon_{z^2}, \epsilon_{zx}, \epsilon_{x^2-y^2}) = (-0.12, +0.10, -0.19, +0.10, +0.16)$ eV.

t (LaFeAsO)	xy	yz	z^2	zx	x^2-y^2
xy	-0.32	-0.25	-0.30	-0.25	0.00
yz	-0.25	-0.21	-0.08	-0.13	0.18
z^2	-0.30	-0.08	0.08	-0.08	0.00
zx	-0.25	-0.13	-0.08	-0.21	-0.18
x^2-y^2	0.00	0.18	0.00	-0.18	-0.18
U (LaFeAsO)	xy	yz	z^2	zx	x^2-y^2
xy	3.31	1.95	1.89	1.95	2.09
yz	1.95	2.77	2.20	1.78	1.67
z^2	1.89	2.20	3.27	2.20	1.65
zx	1.95	1.78	2.20	2.77	1.67
x^2-y^2	2.09	1.67	1.65	1.67	2.20
J (LaFeAsO)	xy	yz	z^2	zx	x^2-y^2
xy	-	0.54	0.64	0.54	0.27
yz	0.54	-	0.41	0.45	0.43
z^2	0.64	0.41	-	0.41	0.50
zx	0.54	0.45	0.41	-	0.43
x^2-y^2	0.27	0.43	0.50	0.43	-
t (LaFePO)	xy	yz	z^2	zx	x^2-y^2
xy	-0.35	-0.31	-0.32	-0.31	0.00
yz	-0.31	-0.24	-0.04	-0.13	0.18
z^2	-0.32	-0.13	0.13	-0.04	0.00
zx	-0.31	-0.13	-0.04	-0.24	-0.18
x^2-y^2	0.00	0.18	0.00	-0.18	-0.27

values (~ 4 eV or larger) employed in model studies,^{19,20} which, as a first look, suggests that much smaller correlation effects should be expected in reality. However, it should be cautioned that the DMFT employed in the literature^{19,20} ignoring spatial correlations may largely underestimate correlation effects. By considering the ratio $U/t \sim 10$ (the value itself is comparable to the cuprates) and the presence of the five-degenerate orbitals per Fe site, electron correlations in these compounds are *moderately* strong. In addition, the present U values have orbital dependence with the order of 1 eV, which will generate nonnegligible orbital dependence of renormalization factor; it can be a critical parameter that affects the Fermi surface in quasiparticle band structure. Our downfolded effective Hamiltonian thus poses various constraints on modeling of this family of materials and careful analyses by accurate low-energy solvers should be required for reliable discussions of magnetic and superconducting mechanisms.

The effective models for LaFeAsO and LaFePO are basically similar in the band dispersion as well as in the screened Coulomb interaction. A main differences is the band width (see Fig.1) and this point can also be confirmed from t values of LaFePO somewhat larger than those of LaFeAsO (see Table I). Another difference is a band close to the Fermi surface at Γ point; i.e., whether it has a two-dimensional dispersion with the $d_{x^2-y^2}$ character or it has a three-dimensional one with the d_{z^2} charac-

ter. These differences can be systematically understood in terms of the Fe-Fe and Fe-pnictogen distances.³⁵ On the other hand, in our calculations, the interaction parameters do not exhibit noticeable differences between LaFeAsO and LaFePO. The mechanism of the superconductivity has to clarify how these subtle differences in the one-body and many-body terms of the effective Hamiltonian lead to a large difference in the critical temperature, 26-55 K for As compounds and 4 K for P compounds.

The present model may be used for further studies by using low-energy solvers such as the dynamical mean-field theory³⁶ and path-integral renormalization group.^{37,38} Our ten-band model may also offer a firm starting point for further downfolding to derive effective models with fewer number of bands near the Fermi level.

This work is supported from MEXT Japan under the grant numbers 16076212, 17071003, 17064004, 19019012, and 19014022. We also thank the facilities at the Supercomputer Center, Institute for Solid State Physics, University of Tokyo. We thank Yoshihide Yoshimoto, Taichi Kosugi, and Takashi Miyake for useful discussions.

- 1) Y. Kamihara, T. Watanabe, M. Hirano and H. Hosono: J. Am. Chem. Soc. **130** (2008) 3296.
- 2) Z. A. Ren, W. Lu, J. Yang, W. Yi, X. L. Shen, Z. C. Li, G. C. Che, X. L. Dong, L. L. Sun, F. Zhou, Z. X. Zhao: arXiv:0804.2053v1.
- 3) C. de la Cruz, Q. Huang, J. W. Lynn, J. Li, W. Ratcliff II, J. L. Zarestky, H. A. Mook, G. F. Chen, J. L. Luo, N. L. Wang and P. Dai: Nature **453** (2008) 899.
- 4) Z. A. Ren, G. C. Che, X. L. Dong, J. Yang, W. Lu, W. Yi, X. L. Shen, Z. C. Li, L. L. Sun, F. Zhou, Z. X. Zhao: arXiv:0804.2582v1.
- 5) Y. Nakai, K. Ishida, Y. Kamihara, M. Hirano and H. Hosono: J. Phys. Soc. Jpn. **77** (2008) 073701; K. Ahilan, F. L. Ning, T. Imai, A. S. Sefat, R. Jin, M. A. McGuire, B. C. Sales, D. Mandrus: arXiv:0804.4026v2.
- 6) J. P. Carlo, Y. J. Uemura, T. Goko, G. J. MacDougall, J. A. Rodriguez, W. Yu, G. M. Luke, P. Dai, N. Shannon, S. Miyasaka, S. Suzuki, S. Tajima, G. F. Chen, W. Z. Hu, J. L. Luo, N. L. Wang: arXiv:0805.2186v1.
- 7) T. Sato, S. Souma, K. Nakayama, K. Terashima, K. Sugawara, T. Takahashi, Y. Kamihara, M. Hirano and H. Hosono: J. Phys. Soc. Jpn. **77** (2008) 063708; Y. Ishida, R. Eguchi, M. Matsunami, K. Horiba, M. Taguchi, A. Chainani, Y. Senba, H. Ohashi, H. Ohta, S. Shin: arXiv:0712.3083.
- 8) H. Liu, X. Jia, W. Zhang, L. Zhao, J. Meng, G. Liu, X. Dong, G. Wu, R. H. Liu, X. H. Chen, Z. A. Ren, W. Yi, G. C. Che, G. F. Chen, N. L. Wang, G. Wang, Y. Zhou, Y. Zhu, X. Wang, Z. Zhao, Z. Xu, C. Chen, X. J. Zhou: arXiv:0805.3821v1.
- 9) Y. Kamihara, H. Hiramatsu, M. Hirano, R. Kawamura, H. Yanagi, T. Kamiya, and H. Hosono: J. Am. Chem. Soc. **128** (2006) 10012.
- 10) D. J. Singh and M. H. Du: arXiv:0803.0429v1.
- 11) C. Cao, P. J. Hirschfeld, and H. P. Cheng: arXiv:0803.3236v1
- 12) S. Ishibashi, K. Terakura and H. Hosono: J. Phys. soc. Jpn. **77** (2008) 053709.
- 13) F. Ma and Z. Y. Lu: arXiv:0803.3286v1.
- 14) K. Kuroki, S. Onari, R. Arita, H. Usui, Y. Tanaka, H. Kontani, H. Aoki: arXiv:0803.3325v1.
- 15) I. I. Mazin, M. D. Johannes, L. Boeri, K. Koepernik, D. J. Singh: arXiv:0806.1869v1.
- 16) I. I. Mazin, D. J. Singh, M. D. Johannes, M. H. Du: arXiv:0803.2740v2.
- 17) J. Dong, H. J. Zhang, G. Xu, Z. Li, G. Li, W. Z. Hu, D. Wu, G. F. Chen, X. Dai, J. L. Luo, Z. Fang, N. L. Wang: arXiv:0803.3426v1.
- 18) T. Yildirim: arXiv:0804.2252v1.
- 19) A. O. Shorikov, M. A. Korotin, S. V. Streltsov, S. L. Skornyakov,

- D. M. Korotin, V. I. Anisimov: arXiv:0804.3283v1.
- 20) K. Haule, J. H. Shim, and G. Kotliar: Phys. Rev. Lett. **100** (2008) 226402.
- 21) L. Craco, M. S. Laad, S. Leoni and H. Rosner: arXiv:0805.3636v1
- 22) F. Aryasetiawan, M. Imada, A. Georges, G. Kotliar, S. Biermann, and A. I. Lichtenstein: Phys. Rev. B **70** (2004) 195104.
- 23) I. V. Solovyev and M. Imada: Phys. Rev. B **71** (2005) 045103.
- 24) Y. Imai, I. Solovyev, and M. Imada: Phys. Rev. Lett. **95** (2005) 176405; Y. Imai and M. Imada: J. Phys. Soc. Jpn. **75** (2006) 094713.
- 25) Y. Otsuka and M. Imada: J. Phys. Soc. Jpn. **75** (2006) 124707.
- 26) K. Nakamura, Y. Yoshimoto, R. Arita, S. Tsuneyuki, and M. Imada: Phys. Rev. B **77** (2008) 195126.
- 27) N. Marzari and D. Vanderbilt: Phys. Rev. B **56** (1997) 12847; I. Souza, N. Marzari and D. Vanderbilt: Phys. Rev. B **65** (2002) 035109.
- 28) O. Gunnarsson, O. K. Andersen, O. Jepsen, and J. Zaanen: Phys. Rev. B **39** (1989) 1708.
- 29) F. Aryasetiawan, K. Karlsson, O. Jepsen, and U. Schonberger: Phys. Rev. B **74** (2006) 125106; T. Miyake and F. Aryasetiawan: Phys. Rev. B **77** (2008) 085122.
- 30) M. Tsukada *et al.*, computer program package TAPP, University of Tokyo, Tokyo, JAPAN, 1983–2000: J. Yamauchi, M. Tsukada, S. Watanabe, and O. Sugino: Phys. Rev. B **54** (1996) 5586.
- 31) J. P. Perdew, K. Burke, and M. Ernzerhof: Phys. Rev. Lett. **77** (1996) 3865.
- 32) N. Troullier and J. L. Martins: Phys. Rev. B **43** (1991) 1993.
- 33) L. Kleinman and D. M. Bylander: Phys. Rev. Lett. **48** (1982) 1425.
- 34) M. S. Hybertsen and S. G. Louie: Phys. Rev. B **34** (1986) 5390; Phys. Rev. B **35** (1987) 5585.
- 35) V. Vildosola, L. Pourovskii, R. Arita, S. Biermann, and A. Georges: arXiv:0806.3285v1
- 36) A. Georges, G. Kotliar, W. Krauth and M. J. Rozenberg: Rev. Mod. Phys. **68** (1996) 13.
- 37) M. Imada and T. Kashima: J. Phys. Soc. Jpn. **69** (2000) 2723.
- 38) T. Kashima and M. Imada: J. Phys. Soc. Jpn. **70** (2001) 2287.